Atmos. Chem. Phys. Discuss., 10, 6895–6921, 2010
www.atmos-chem-phys-discuss.net/10/6895/2010/

Atmospheric Chemistry and Physics Discussions

This discussion paper is/has been under review for the journal Atmospheric Chemistry and Physics (ACP). Please refer to the corresponding final paper in ACP if available.

Dicarboxylic acids, metals and isotopic compositions of C and N in atmospheric aerosols from inland China: implications for dust and coal burning emission and secondary aerosol formation

G. Wang[1], M. Xie[2], S. Hu[2], E. Tachibana[3], and K. Kawamura[3]

[1]State Key Laboratory of Loess and Quaternary Geology, Institute of Earth Environment, Chinese Academy of Sciences, Xi'an 710075, China
[2]State Key Laboratory of Pollution Control and Resources Reuse, Nanjing University, Nanjing 210093, China
[3]Institute of Low Temperature Science, Hokkaido Unversity, Sapporo 060-0819, Japan

Received: 4 February 2010 – Accepted: 28 February 2010 – Published: 11 March 2010

Correspondence to: G. Wang (wanggh@ieecas.cn)

Published by Copernicus Publications on behalf of the European Geosciences Union.

Abstract

Dicarboxylic acids (C_2-C_{10}), metals, elemental carbon (EC), organic carbon (OC), and stable isotopic compositions of total carbon (TC) and total nitrogen (TN) were determined for PM_{10} samples collected at three urban and one suburban sites of Baoji, an inland city of China, during winter and spring 2008. Oxalic acid (C_2) was the dominant diacid, followed by succinic (C_4) and malonic (C_3) acids. Total diacids in the urban and suburban areas are 1546±203 and 1728±495 ng m^{-3} during winter and 1236±335 and 1028±193 ng m^{-3} during spring. EC in the urban and the suburban atmospheres are 17±3.8 and 8.0±2.1 µg m^{-3} during winter and 20±5.9 and 7.1±2.7 µg m^{-3} during spring whereas OC at the urban and suburban sites are 74±14 and 51±7.9 µg m^{-3} in winter and 51±20 and 23±6.1 µg m^{-3} in spring. Secondary organic carbon (SOC) accounted for 38±16% of OC in winter and 28±18% of OC in spring, suggesting an enhanced photochemical production of secondary organic aerosols in winter under an inversion layer development. Total metal elements in winter and spring are 34±10 and 61±27 µg m^{-3} in the urban air and 18±7 and 32±23 µg m^{-3} in the suburban air. A linear correlation (r^2>0.8 in winter and r^2>0.6 in spring) was found between primary organic carbon (POC) and Ca^{2+}/Fe, together with a strong dependence of pH value on water-soluble inorganic carbon, suggesting fugitive dust as a major source of the airborne particles. Polycyclic aromatic hydrocarbons (PAHs), sulfate, and Pb in the samples well correlated each other (r^2>0.6) in winter samples, suggesting an importance of emissions from coal burning for house heating. Stable carbon isotope compositions of TC ($\delta^{13}C$) became higher with an increase in the concentration ratios of C_2/OC due to aerosol aging. In contrast, nitrogen isotope compositions of TN ($\delta^{15}N$) became lower with an increases in the mass ratios of NH_4^+/PM_{10} and NO_3^-/PM_{10} due to an enhanced adsorption and/or condensation of NH_3 and HNO_3 from gas phase onto solid phase.

ACPD
10, 6895–6921, 2010

1 Introduction

Coal is a major energy source in China, accounting for around 70% of the total energy consumption. In 2007, China produced 2.5 billion tons of coal, of which around 50% was burned for generating electricity. A substantial fraction of the remaining is used for domestic heating and cooking. The latter emits a huge amount of carbonaceous aerosols due to low combustion efficiency. These carbonaceous particles, together with sulfate, nitrate and ammonium, can be transported into the North Pacific region and even into North America, causing an inter-continental pollution (Heald et al., 2006).

Very few studies have been performed for air pollution problems in western regions of China, which are characterized by semi-arid/arid climate, intensive usage of coal and relatively lower level of economic development. These situations cause the concentration levels of airborne particulate matter much higher than those in the coastal region of China (Shen et al., 2009; Wang et al., 2006a, b). High concentration of fugitive dust frequently occurs in the western area due to the proximity of dust source regions. Annual average pH values of rainwater were observed with the highest (pH=8.20) in Jiayuguan, a mid-scale city in Northwestern China, and the lowest (pH=3.05) in Jieshou, a mid-scale city in Southern China (China Ministry of Environment Protection, 2006), suggesting that the atmospheric environment in the northwest is different from that in other regions of the country.

Baoji is a mid-scale city (33°35′~35°06′ N, 106°18′~108°03′ E, population 0.8 million) located in the semi-arid region of Northwest China, where high loading of particles has been a persistent air pollution problem because of emissions from coal burning and dust. In order to better understand the impact of coal burning and fugitive dust on the atmosphere over in inland regions of China, an intensive aerosol (PM_{10} and size-segregated particles) sampling was simultaneously conducted at four sites in Baoji city during 2008 winter and spring (Wang et al., 2009, 2010; Xie et al., 2009). Here we reported the chemical compositions of the PM_{10} samples (i.e., dicarboxylic acids, water-soluble inorganic and organic carbon, elemental and organic carbon, and metals) and

ACPD
10, 6895–6921, 2010

their stable carbon and nitrogen isotope compositions, and discussed the characteristics and sources of those airborne particulate matters in the inland region.

2 Experimental section

2.1 Aerosols collection

PM_{10} aerosols were simultaneously collected at three urban sites and one suburban site in Baoji city using a mid-volume air sampler (Laoshan Company, China) at a flow rate of 100 L min^{-1}. The particles were collected onto a pre-baked (450 °C for 12 h) quartz fiber filter (Φ 90 mm). The wintertime sampling was performed on 10–15 February 2008, and the springtime sampling was conducted on 1–6 April 2008. Field blank filter was mounted onto the sampler for a few minutes without sucking the air. The filed blank samples were collected before and after sampling at each site in each season. After sampling, the sample and blank filters were sealed in an aluminum foil and stored at –20 °C prior to analysis.

2.2 Dicarboxylic acids

Analytical method for diacids was reported elsewhere (Kawamura and Ikushima, 1993; Wang et al., 2002). Briefly, an aliquot of the filter was cut in pieces and extracted with pure water. The extracts were concentrated in dryness using a rotary evaporater under a vacuum and then reacted with 10% of BF_3 in butanol at 100 °C for 30 min to convert the carboxyl group into butyl esters. n-Hexane was added to the reaction products and the derivatives were washed with pure water 3 times. Finally, the derivatives in hexane were concentrated into 100 µL and quantified by GC/MS and GC.

ACPD
10, 6895–6921, 2010

2.3 Water-soluble organic carbon (WSOC), water-soluble inorganic carbon (WSIC), elemental carbon (EC), organic carbon (OC) and metal elements

Aliquot of the filter was extracted with pure water. The extracts were determined for pH using a pH meter, and then measured for WSOC and WSIC using a Shimazdu TOC-5000 analyzer (Wang et al., 2003). For the determination of metals, an aliquot of the filter was cut in pieces and digested by $HClO_4$ and HF. Metals in the solution were determined using ICP-AES.

EC and OC in the samples were measured by a Sunset Lab Carbon Analyzer following the Interagency Monitoring of Protected Visual Environments (IMPROVE) thermal protocol (Wang et al., 2005). Briefly, a small disk (area ~1.5 cm^2) of the sample filter was put in a quartz boat inside the analyzer. OC was determined in a helium atmosphere at 120, 250, 450, and 550 °C. Afterwards, oxygen (2%) was introduced and EC was determined from 550 to 900 °C. A He-Ne laser was used to monitor and correct for pyrolytic conversion of OC to EC. Primary organic carbon (POC) and secondary organic carbon (SOC) was calculated using the EC tracer method (Castro et al., 1999; Chu, 2005; Yu et al., 2009).

$$\mathrm{POC} = \mathrm{EC} \cdot \left(\frac{\mathrm{OC}}{\mathrm{EC}}\right) \mathrm{min}, \quad \text{(R1)}$$

$$\mathrm{SOC} = \mathrm{OC} - \mathrm{POC} \quad \text{(R2)}$$

2.4 Total carbon (TC), total nitrogen (TN) and stable isotopic compositions of TC and TN

For TC and TN measurements, a small disk of sample filter was placed in a tin cup and combusted at 1400 °C using an elemental analyzer (EA) (Carlo Erba, EA 1500). The derived NO was converted into N_2 in a reduction column. N_2 and CO_2 gases were isolated on a GC in EA and determined with a thermal conductivity detector (Kawamura

et al., 2003). Stable isotope composition of TC and TN were conducted using the same EA interfaced to isotope ratio mass spectrometer (IRMS) (ThermoQuest, Delta Plus) (Narukawa et al., 1999). Inorganic ions in the samples are reported elsewhere (Wang et al., 2010) and cited here for calculating organic nitrogen (ON) in PM_{10}. NO_3^- and NH_4^+ are the major inorganic species containing nitrogen while NO_2^- is negligible, thus ON concentration can be calculated as follow:

$$ON = TN - 14 \cdot \left(\frac{[NO_3^-]}{62} + \frac{[NH_4^+]}{18} \right) \quad \text{(R3)}$$

3 Results and discussion

3.1 Particle mass, EC, OC, TC and TN

Table 1 shows the seasonal variations of major species in the samples at the urban and suburban sites. A similar level of PM_{10} concentrations was observed in winter and spring, but the pH of the water-extracted solution was lower in winter (pH=6.1±0.6) than in spring (pH=7.0±0.4), indicating the wintertime PM_{10} is more acidic. Moreover, the suburban samples showed lower pH values compared to those of urban samples due to an enhanced deposition of dust, being consistent with the spatial distribution of water-soluble inorganic carbon (WSIC). A strong correlation was found between pH of the water-extracts and WSIC in the samples; the pH values increase when WSIC concentrations increase in both seasons (Fig. 1). Such a strong relation, however, was not observed between the pH and sulfate at the same sites (Wang et al., 2010), suggesting that the acidity of airborne particles in inland China is controlled by dust-/soil-derived species rather than sulfate. Water-soluble organic carbon (WSOC) showed a similar level at the urban (31±6.9 $\mu g\,m^{-3}$) and suburban (31±3.4 $\mu g\,m^{-3}$) sites during winter, which are 1.5 times higher than those during spring (Table 1). Organic carbon (OC) is more abundant in winter than in spring, and also more abundant in the urban regions

than in the suburban area. It may be due to more emissions of fossil fuel combustion at the urban area, especially in winter when burning coal for house heating is very common. Elemental carbon (EC) in the urban aerosols is 17±3.8 μg m^{-3} in winter and 20±5.9 μg m^{-3} in spring, being 2–3 times higher than those at the suburban sites.

During winter OC/EC ratios are 4.5±0.9 in the urban and 6.5±0.9 in the suburban sites. On the other hands, OC/EC ratios in spring are 2.7±0.7 and 3.4±0.7 in the urban and suburban areas, respectively (Fig. 2). The higher OC/EC ratios in winter mainly resulted from emissions from residential coal burning for house heating, which contain more organic pollutants compared with vehicle exhausts (Cao et al., 2005). In contrast, higher ratios of OC/EC in the suburban region are mainly caused by more biogenic emissions. Relative abundance of WSOC in OC is 43±9% in urban site and 60±3% in suburban site in winter whereas they are 46±24% and 73±25% at both sites in spring (Fig. 2). Organic matter (OM), which was calculated by multiplying OC by a factor of 1.6 (Turpin and Lim, 2001), accounted for more than 25% of PM_{10} mass in winter and less than 20% of the particle mass in spring due to an enhanced input of dust in the warm season. Compared to OM, EC is relatively minor component, accounting for less than 5% of the particle mass. The sum of OM and EC accounts for 30% of PM_{10} in winter and 20% of PM_{10} in spring, suggesting that inorganic components are the major fraction of the particles in inland China.

Figure 3 shows the seasonal and spatial variations of POC and SOC in the city. Wintertime POC is 48±11 μg m^{-3} at the urban sites, which is approximately two times higher than that (23±6 μg m^{-3}) at the suburban site. In contrast, SOC of the urban samples is equivalent to that of the suburban particles. In spring, POC and SOC are 37±11 and 14±10 μg m^{-3} in the urban air and 14±5 and 9±3 μg m^{-3} in the suburban atmosphere, respectively. SOC/POC ratios for the urban and suburban samples are 0.6±0.3 and 1.3±0.3 during winter and 0.4±0.4 and 0.8±0.3 during spring. The higher SOC/POC ratios in winter suggest an enhanced photo-oxidation of organics under favorable meteorological conditions (e.g., a development of inversion layer) (Yu et al., 2009). Furthermore, the higher SOC/POC ratios at the suburban site also indicate an

increased photochemical production during the transport process of organic pollutants from the urban to the suburban.

Total nitrogen (TN) and organic nitrogen (ON) showed a similar concentration level in the urban and suburban samples with TN being 2–5 times higher than ON (Table 1), indicating that organic nitrogen species in inland China are relatively minor.

3.2 Dicarboxylic acids, glyoxylic acid and metals

Homologs of dicarboxylic acids (C_2-C_{10}) were detected in the samples with oxalic acid (C_2) being most abundant followed by succinic (C_4) and malonic (C_3) acids. Concentration of oxalic acid (C_2) was 816±172 ng m^{-3} in the urban samples and 984±373 ng m^{-3} in the suburban samples during winter whereas its spring concentration was 532±247 ng m^{-3} at the urban sites and 413±154 ng m^{-3} at the suburban site (Table 2). These values are comparable to those reported in Nanjng (178–1388 ng m^{-3}, av. 790 ng m^{-3}) (Wang et al., 2002) and other 14 Chinese mega-cities (151–1437 ng m^{-3}, av. 558 ng m^{-3}) (Ho et al., 2007). Concentration of glyoxylic acid, a smallest keto-carboxylic acid, is 283±135 and 289±58 ng m^{-3} in the urban and suburb samples in winter and 95±30 and 101±41 ng m^{-3} in spring, around 10 times more abundant than that (38±20 ng m^{-3} in winter) in Chinese mega-cities (Ho et al., 2007). As shown in Fig. 4, C_3/C_2 ratio linearly correlated with that of C_4/C_2 in both seasons. Such a strong correlation suggests that C_3 and C_4 may be the major precursors of C_2 (Wang and Kawamura, 2006).

A total of 18 metals were determined in the samples with Ca being the most abundant, followed by Al, Fe, K, Mg and Na. Other metals such as Cd, Co, Cu, Ni and V are minor (Table 2). A strong correlation was found for the crustal elements, i.e., Al, Ba, Ca, Fe, K, Mg and Ti ($r \geq 0.76$ for the winter samples and $r \geq 0.83$ for the spring samples, Tables 3 and 4). Those components are also significantly correlated with Ca^{2+} (Tables 3 and 4). Total metals determined are 34±10 and 18±7 μg m^{-3} in the urban and suburban atmospheres during winter, respectively. These values are around 50%

of those in springtime (Table 2), demonstrating an increased input of dust in the inland city during spring.

3.3 Mass closure of PM_{10}

To reconstruct the sample mass balance, the metals were converted as their oxide forms while OC was converted into OM as mentioned above. The reconstructed concentrations and percentages of the determined species are shown in Fig. 5 and Table 5. The most abundant species in the particles are OM, accounting for around one fourth of PM_{10} mass in winter and one sixth of the particle mass in spring, followed by SO_4^{2-}, NO_3^-, NH_4^+, metal oxides and EC (Table 5). The sum of all the quantified components including EC, OM, inorganic ions and metal oxides accounted for more than 70% of the PM_{10} mass in winter and 60% of the particle mass in spring with the remaining mostly being silicon-related components (Table 5).

3.4 Implications for dust and coal burning emission and secondary aerosol formation

A strong linear correlation was found between POC and Fe (Fig. 6a) and between POC and Ca^{2+} (Fig. 6b), suggesting that POC in the PM_{10} largely originated from soil dust. Such a linear correlation in turn demonstrates that the approach we used for the differentiation of POC and SOC from OC is useful. In the previous studies we found that sulfate and PAHs in the PM_{10} samples mostly resulted from coal burning emissions (Xie et al., 2009; Wang et al., 2010). In the current study we further observed a linear correlation between Pb with sulfate (Fig. 7a and b) and PAHs (Fig. 7c and d). Like sulfate Pb is largely derived from coal burning, thus the linear correlation of Pb with sulfate and PAHs again confirms the importance of coal-burning smoke as a major source.

ACPD
10, 6895–6921, 2010

Oxalic acid (C_2) is mostly formed via photochemical oxidation of various organic precursors including glyoxylic acid, although a small fraction of C_2 can be directly emitted from vehicle exhaust (Kawamura and Kaplan, 1987; Kawamura and Yasui, 2005). Thus the concentration ratio of C_2/OC can be thought as an indicator of aerosol aging, that is, higher ratio of C_2/OC means aerosol is more aged. Oxidation processes in general result in fractionation between the heavy and light isotopes favoring the light isotope to accumulate in the product (Hoefs, 1997; Sakugawa and Kaplan, 1995). Although the reactant enriches with the heavy isotopes, compounds formed from oxidation processes in the atmosphere are isotopically lighter due to the kinetic isotope effect (KIE) (Fisseha et al., 2009; Wang and Kawamura, 2006). In the current study we found that δ^{13}C of TC became higher with an increase in the ratio of C_2/OC (Fig. 8a and b). C_2 is formed by oxidation of C_3, C_4 and other precursors. During the further atmospheric oxidation process, i.e., removal of CO_2/CO by reaction with OH radical, lighter isotope (^{12}C) could be more enriched in the evolved species leaving the remaining substrate more enriched in ^{13}C (Aggarwal and Kawamura, 2009; Wang and Kawamura, 2006). Thus such an enrichment of ^{13}C with an increase in C_2/OC for the PM_{10} samples can be ascribed to aerosol photochemical aging.

Solid-phase NH_4^+ and NO_3^-, however, are formed via adsorption/condensation of gaseous NH_3 and HNO_3 onto pre-existing particles (Seinfeld and Pandis, 1998), favoring an enrichment of light ^{14}N in particles (Hoefs, 1997; Yeatman et al., 2001). Therefore, the decrease in δ^{15}N of TN with an increase in the ratios of NH_4^+/PM_{10} and NO_3^-/PM_{10} can also be attributable to aerosol aging (Fig. 8c–f). Since particulate NH_4^+ and NO_3^- may convert into NH_3 and HNO_3 and subsequently evaporate into the air, resulting in an enrichment of heavy ^{15}N in particles, the decreasing trend of δ^{15}N of TN further suggests that the adsorption/condensation of gaseous NH_3 and HNO_3 onto pre-existing particles overwhelm the decomposition and evaporation of solid-phase NH_4^+ and NO_3^-.

ACPD
10, 6895–6921, 2010

4 Summary and conclusion

Winter and spring PM_{10} samples from Baoji, an inland city of China, were chemically characterized for water-soluble organic species and metals. Oxalic acid (C_2) is the most abundant diacid, followed by succinic (C_4) and malonic (C_3) acids. Concentrations of dicarboxylic and glyoxylic acids are 1776±543 and 1185±316 ng m^{-3} in winter and spring with no significant difference between the urban and suburban sites. EC in the urban and the suburban atmospheres are 17±3.8 and 8.0±2.1 µg m^{-3} during winter and 20±5.9 and 7.1±2.7 µg m^{-3} during spring whereas OC at the urban and suburban sites are 74±14 and 51±7.9 µg m^{-3} in winter and 51±20 and 23±6.1 µg m^{-3} in spring. SOC/POC ratios are higher in winter than in spring, indicating an enhanced photochemical oxidation in the cold season under a development of inversion layer. pH of water-extracted solution of the samples showed a strong correlation (r^2>0.8) with WSIC, suggesting fugitive dust as the major source of airborne particles in the city. Moreover, POC also showed a linear correlation (r^2>0.8 in winter and r^2>0.6 in spring) with Ca^{2+} and Fe, further confirming the importance of fugitive dust. C_3/C_2 ratio positively correlated with C_4/C_2 ratio, probably indicating C_3 and C_4 as the precursors of C_2. PAHs, sulfate, and Pb in the samples correlated each other with r^2>0.6 for winter samples, suggesting an importance of coal burning emissions due to house heating. $\delta^{13}C$ of TN increased with an increase in the concentration ratio of C_2/OC, which is mostly due to aerosol aging. In contrast, $\delta^{15}N$ of TC decreased as an increase in the ratios of NH_4^+/PM_{10} and NO_3^-/PM_{10} due to the absorption/condensation of gaseous NH_3 and HNO_3 onto pre-existing particles.

Acknowledgements. This work was financially supported by National Natural Science Foundation (No. 40873083) and the Knowledge Innovation Program of Chinese Academy Sciences, China (No. kzcx2-yw-148).

References

Aggarwal, S. G. and Kawamura, K.: Carbonaceous and inorganic composition in long-range transported aerosols over northern Japan: Implication for aging of water-soluble organic fraction, Atmos. Environ., 43, 2532–2540, 2009.

Cao, J. J., Wu, F., Chow, J. C., Lee, S. C., Li, Y., Chen, S. W., An, Z. S., Fung, K. K., Watson, J. G., Zhu, C. S., and Liu, S. X.: Characterization and source apportionment of atmospheric organic and elemental carbon during fall and winter of 2003 in Xi'an, China, Atmos. Chem. Phys., 5, 3127–3137, 2005, http://www.atmos-chem-phys.net/5/3127/2005/.

Castro, L. M., Pio, C. A., Harrison, R. M., and Smith, D. J. T.: Carbonaceous aerosol in urban and rural European atmospheres: estimation of secondary organic carbon concentrations, Atmos. Environ., 33, 2771–2781, 1999.

China Ministry of Environment Protection: Annual report of China Environment in 2004, China Ministry of Environment Protection, Beijing, 2006.

Fisseha, R., Spahn, H., Wegener, R., Hohaus, T., Brasse, G., Wissel, H., Tillmann, R., Wahner, A., and Koppmann, R.: Stable carbon isotope composition of secondary organic aerosol from b-pinene oxidation, J. Geophys. Res.-Atmos., 114, D02304, doi:10.1029/2008JD011326, 2009.

Heald, C. L., Jacob, D. J., Park, R. J., Alexander, B., Fairlie, T. D., Yantosca, R. M., and Chu, D. A.: Transpacific transport of Asian anthropogenic aerosols and its impact on surface air quality in the United States, J. Geophys. Res., 111, D14310, doi:10.1029/2005JD006847, 2006.

Ho, K. F., Cao, J. J., Lee, S. C., Kawamura, K., Zhang, R. J., Chow, J. C., and Watson, J. G.: Dicarboxylic acids, ketocarboxylic acids, and dicarbonyls in the urban atmosphere of China, J. Geophys. Res.-Atmos., 112, D22S27, doi:1029/2006JD008011, 2007.

Hoefs, J.: Stable Isotope Geochemistry, Springer, New York, 1997.

Kawamura, K. and Ikushima, K.: Seasonal changes in the distribution of dicarboxylic acids in the urban atmosphere, Environ. Sci. Technol., 27, 2227–2235, 1993.

Kawamura, K. and Kaplan, I. R.: Motor exhaust emissions as a primary source for dicarboxylic acids in Los Angeles ambient air, Environ. Sci. Technol., 21, 105–110, 1987.

Kawamura, K. and Yasui, O.: Diurnal changes in the distribution of dicarboxylic acids, ketocarboxylic acids and dicarbonyls in the urban Tokyo atmosphere, Atmos. Environ., 39, 1945–1960, 2005.

Narukawa, M., Kawamura, K., Takeuchi, N., and Nakajima, T.: Distribution of dicarboxylic acids and carbon isotopic compositions in aerosols from 1997 Indonesian forest fires, Geophys. Res. Lett., 26, 3101–3104, 1999.

Sakugawa, H. and Kaplan, I. R.: Stable carbon-isotope measurements of atmospheric organic acids in Los Angeles, California, Geophys. Res. Lett., 22, 1509–1512, 1995.

Seinfeld, J. H. and Pandis, S. N.: Atmospheric Chemistry and Physics, John Wiley & Sons, New York, 1998.

Shen, Z., Cao, J., Arimoto, R., Han, Z., Zhang, R., Han, Y., Liu, S., Okuda, T., Nakao, S., and Tanaka, S.: Ionic composition of TSP and PM2.5 during dust storms and air pollution episodes at Xi'an, China, Atmos. Environ., 2911–2918, 2009.

Turpin, B. J. and Lim, H. J.: Species contributions to PM2.5 mass concentrations: Revisiting common assumptions for estimating organic mass, Aerosol Sci. Tech., 35, 602–610, 2001.

Wang, G., Hu, S., Xie, M., and Zhou, B.: Water-soluble inorganic ions and organic carbon of PM10 aerosols in Baoji, an inland city of China, Atmos. Res., under review, 2010.

Wang, G., Kawamura, K., Xie, M., Hu, S., Gao, S., Cao, J., An, Z., and Wang, Z.: Size-distributions of *n*-alkanes, PAHs and hopanes and their sources in the urban, mountain and marine atmospheres over East Asia, Atmos. Chem. Phys., 9, 8869–8882, 2009, http://www.atmos-chem-phys.net/9/8869/2009/.

Wang, G., Wang, H., Yu, Y., Gao, S., Feng, J., Gao, S., and Wang, L.: Chemical characterization of water-soluble components of PM10 and PM2.5 atmospheric aerosols in five locations of Nanjing, China, Atmos. Environ., 37, 2893–2902, 2003.

Wang, G. H., Kawamura, K., Lee, S. C., Ho, K. F., and Cao, J. J.: Molecular, seasonal and spatial distributions of organic aerosols from fourteen Chinese cities, Environ. Sci. Technol., 40, 4619–4625, 2006a.

Wang, G. H., Kawamura, K., Watanabe, T., Lee, S. C., Ho, K. F., and Cao, J. J.: Heavy loadings and source strengths of organic aerosols in China, Geophys. Res. Lett., 33, L22801, doi:10.1029/2006GL027624, 2006b.

Wang, G. H., Niu, S. L., Liu, C., and Wang, L. S.: Identification of dicarboxylic acids and aldehydes of PM10 and PM2.5 aerosols in Nanjing, China, Atmos. Environ., 36, 1941–1950, 2002.

Wang, H. and Kawamura, K.: Stable carbon isotopic composition of low-molecular-weight dicarboxylic acids and ketoacids in remote marine aerosols, J. Geophys. Res.-Atmos., 111, D07304, doi;10.1029/2005JD006466, 2006.

Wang, H., Kawamura, K., and Shooter, D.: Carbonaceous and ionic components in wintertime atmospheric aerosols from two New Zealand cities: Implications for solid fuel combustion, Atmos. Environ., 39, 5865–5875, 2005.

Xie, M., Wang, G., Hu, S., Han, Q., Xu, Y., and Gao, Z.: Aliphatic and polycyclic aromatic hydrocarbons in atmospheric PM_{10} particles in Baoji, China: Implications for coal burning, Atmos. Res., 93, 840–848, 2009.

Yeatman, S. G., Spokes, L. J., Dennis, P. F., and Jickells, T. D.: Can the study of nitrogen isotopic composition in size-segregated aerosol nitrate and ammonium be used to investigate atmospheric processing mechanism?, Atmos. Environ., 35, 1337–1345, 2001.

Yu, X.-Y., Cary, R. A., and Laulainen, N. S.: Primary and secondary organic carbon downwind of Mexico City, Atmos. Chem. Phys., 9, 6793–6814, 2009, http://www.atmos-chem-phys.net/9/6793/2009/.

Table 1. Concentrations of major components and C and N isotopic composition of PM_{10} in Baoji City, China ($\mu g\,m^{-3}$).

	Winter		Spring	
	Urban (n=15)	Suburban (n=5)	Urban (n=18)	Suburban (n=6)
PM_{10}	433±85	333±71	448±153	296±134
ΔpH[a]	–1.6±0.4	–2.4±0.8	–1.3±0.4	–2.1±0.2
WSIC[b]	1.3±0.4	0.9±0.3	1.8±0.7	1.0±0.3
WSOC[c]	31±6.9	31±3.4	22±11	19±6.3
OC[d]	74±14	51±7.9	51±20	26±8.4
EC[e]	17±3.8	8.0±2.1	20±5.9	7.1±2.7
TC[f]	87±14	54±5.9	73±24	31.2±9.6
TN[g]	54±28	56±19	25±6.3	25±8.3
ON[h]	22±15	22±8.7	5.2±2.3	5.2±3.6
$\delta^{13}C$, ‰	–23.4±0.4	–22.5±0.2	–24.4±0.5	–23.9±0.7
$\delta^{15}N$, ‰	23.1±8.3	8.8±5.7	22.5±1.7	17.5±2.0

[a] ΔpH = pH of sample-pH of blank,
[b] WSIC: water-soluble inorganic carbon,
[c] WSOC: water-soluble organic carbon,
[d] OC: organic carbon,
[e] EC: elemental carbon,
[f] TC: total carbon,
[g] TN: total nitrogen,
[h] ON: organic nitrogen.

ACPD
10, 6895–6921, 2010

Table 2. Concentrations of dicarboxylic acids, aldehyde and elements in PM_{10} of Baoji City, China (ng m^{-3}).

	Winter		Spring	
	Urban (n=15)	Suburban (n=5)	Urban (n=18)	Suburban (n=6)
I. Dicarboxylic acids and Keto acid				
Oxalic acid (C_2)	816±172	984±373	532±247	413±154
Malonic acid (C_3)	219±26	209±11	198±25	191±22
Succinic acid (C_4)	255±40	288±78	216±30	202±24
Glutaric acid (C_5)	109±13	111±15	101±11	93±3
Adipic acid (C_6)	26±29	30±35	53±21	44±22
Pimelic acid (C_7)	Nd[f]	Nd[f]	Nd[f]	Nd[f]
Suberic acid (C_8)	Nd[f]	Nd[f]	Nd[f]	Nd[f]
Azelaic acd (C_9)	120±32	106±25	136±57	85±6
Decanedioic acid (C_{10})	Nd[f]	Nd[f]	Nd[f]	Nd[f]
Glyoxylix acid (ωC_2)	283±135	289±58	95±30	101±41
Subtotal	1829±304	2107±541	1332±354	1129±229
II. Metals				
Al	8678±2521	4841±2314	13 840±6319	8352±6715
Ba	174±39	86±26	240±92	108±65
Ca	9779±4071	3610±1606	22 566±11 193	8661±7159
Cd	9±5	5±1	3±7	3±7
Co	6±1	2±1	5±3	3±3
Cr	16±25	20±24	11±22	14±34
Cu	62±20	63±49	56±26	70±22
Fe	5340±1302	2351±749	10 106±4484	4684±3517
K	4016±880	3015±783	5800±2221	3659±2001
Mg	1795±517	974±271	3299±1918	2176±2070
Mn	199±72	120±24	312±121	166±89
Na	2508±1356	1737±1266	1565±2037	1887±2031
Ni	16±13	7±1	21±13	5±5
Pb	612±251	445±172	616±218	469±211
Sr	101±25	44±10	110±55	55±38
Ti	515±111	243±50	742±307	447±259
V	13±3	7±2	14±7	11±8
Zn	791±340	511±75	1208±271	745±208
Subtotal, μg m^{-3}	34±10	18±7	61±27	32±23

ACPD
10, 6895–6921, 2010

Table 3. Correlation coefficients of dust-derived species in PM_{10} during winter (n=20, p=0.01).

	Ca^{2+}	Al	Ba	Ca	Fe	K	Mg	Ti
Ca^{2+}	1.00							
Al	0.85	1.00						
Ba	0.92	0.95	1.00					
Ca	0.88	0.89	0.91	1.00				
Fe	0.91	0.94	0.98	0.95	1.00			
K	0.79	0.80	0.87	0.76	0.79	1.00		
Mg	0.87	0.92	0.95	0.96	0.95	0.83	1.00	
Ti	0.87	0.91	0.91	0.89	0.95	0.67	0.87	1.00

ACPD
10, 6895–6921, 2010

Table 4. Correlation coefficients of dust-derived species in PM_{10} during spring (n=24, p=0.01).

	Ca^{2+}	Al	Ba	Ca	Fe	K	Mg	Ti
Ca^{2+}	1.00							
Al	0.83	1.00						
Ba	0.85	0.87	1.00					
Ca	0.90	0.93	0.94	1.00				
Fe	0.85	0.93	0.92	0.92	1.00			
K	0.87	0.97	0.92	0.96	0.96	1.00		
Mg	0.78	0.98	0.84	0.89	0.90	0.96	1.00	
Ti	0.86	0.97	0.90	0.93	0.95	0.97	0.92	1.00

ACPD
10, 6895–6921, 2010

Table 5. Percentages of major species in particle mass, %.

	Winter		Spring	
	Urban	Suburban	Urban	Suburban
OM	27±3.2	25±2.1	19±3.8	13±3.1
EC	3.9±0.7	2.4±0.3	4.5±0.9	2.5±0.2
NO_3^-	9.3±3.2[a]	14±2.4[a]	7.4±2.4[a]	11±3.6[a]
SO_4^{2-}	11±3.5[a]	14±2.2[a]	7.0±1.9[a]	10±2.1[a]
NH_4^+	6.6±1.6[a]	9.1±0.6[a]	4.0±1.5[a]	6.7±2.1[a]
Ca^{2+}	1.5±0.4[a]	0.8±0.2[a]	2.2±0.4[a]	1.7±0.5[a]
$F^-+Cl^-+Na^++K^++Mg^{2+}$	2.7±0.8[a]	2.9±0.7[a]	3.2±3.0[a]	2.9±1.7[a]
Metal oxides	8.1±2.1	5.5±1.7	13±2.7	10±5.0
Total	70±5.5	73±3.1	60±6.1	588.6

[a] Data were calculated from Wang et al. (2009a).

ACPD
10, 6895–6921, 2010

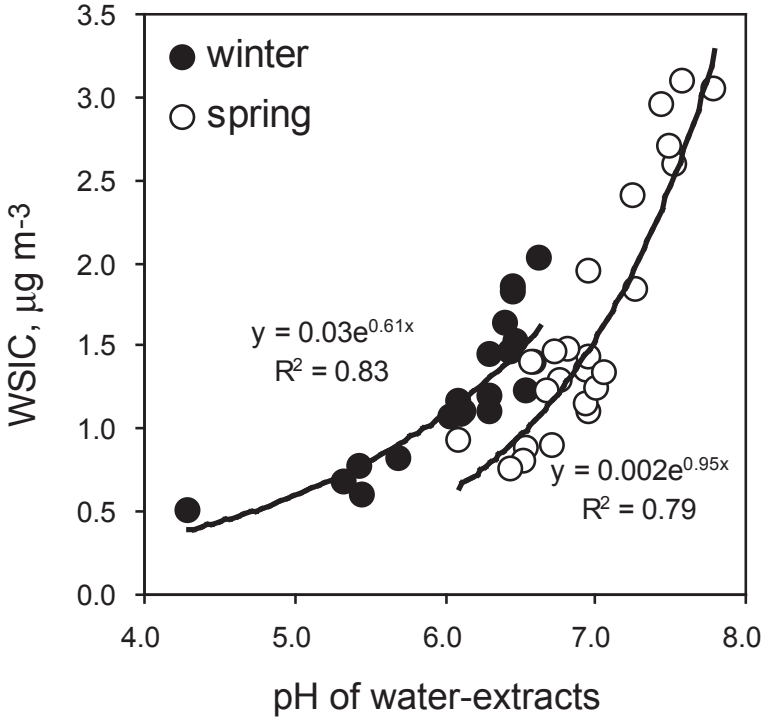

Fig. 1. Correlation of water-soluble inorganic carbon (WSIC) and pH of water-extracts of the PM_{10} samples during winter and spring.

ACPD
10, 6895–6921, 2010

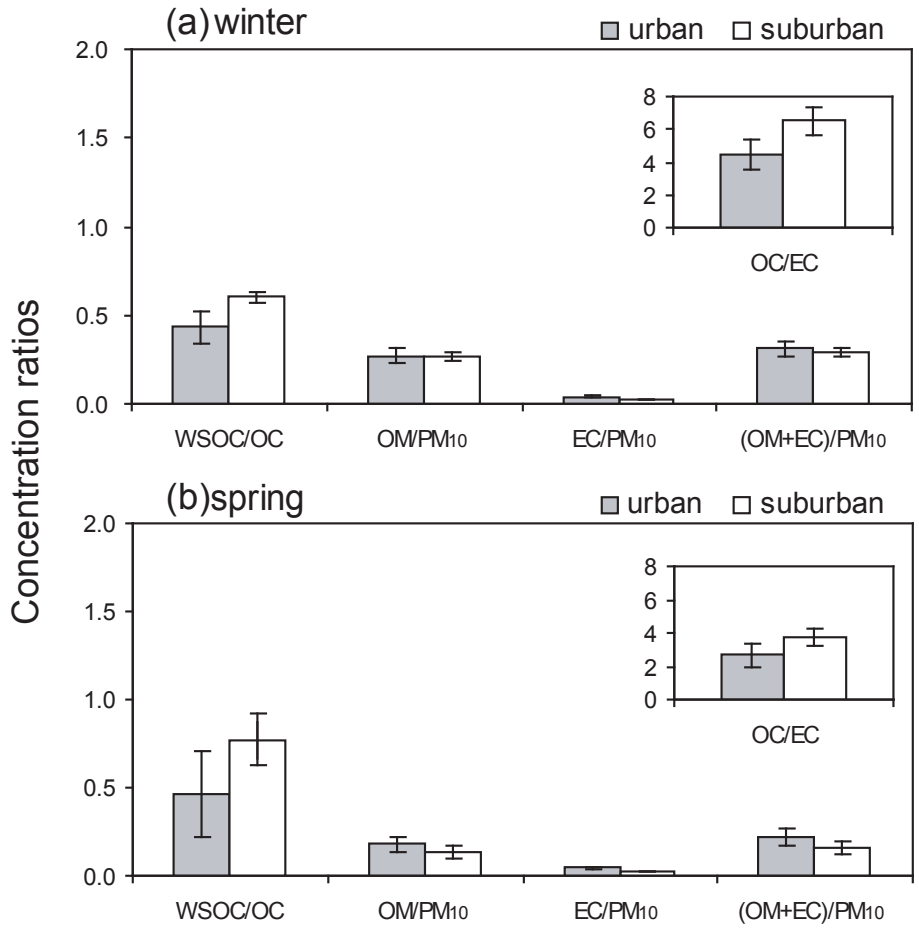

Fig. 2. Relative abundance of major species in the urban and suburban areas of Baoji City during winter and spring.

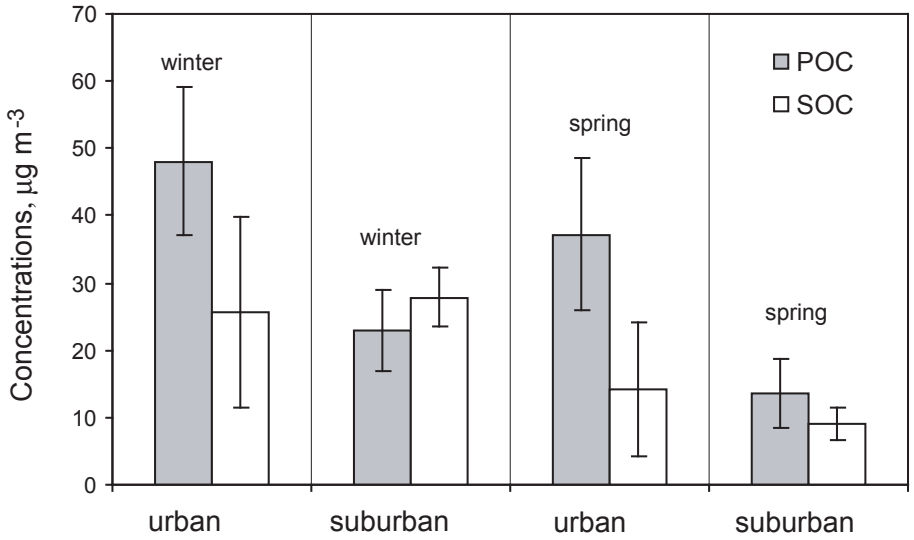

Fig. 3. Concentrations of primary organic carbon (POC) and secondary organic carbon (SOC) in the urban and suburban atmosphere.

ACPD
10, 6895–6921, 2010

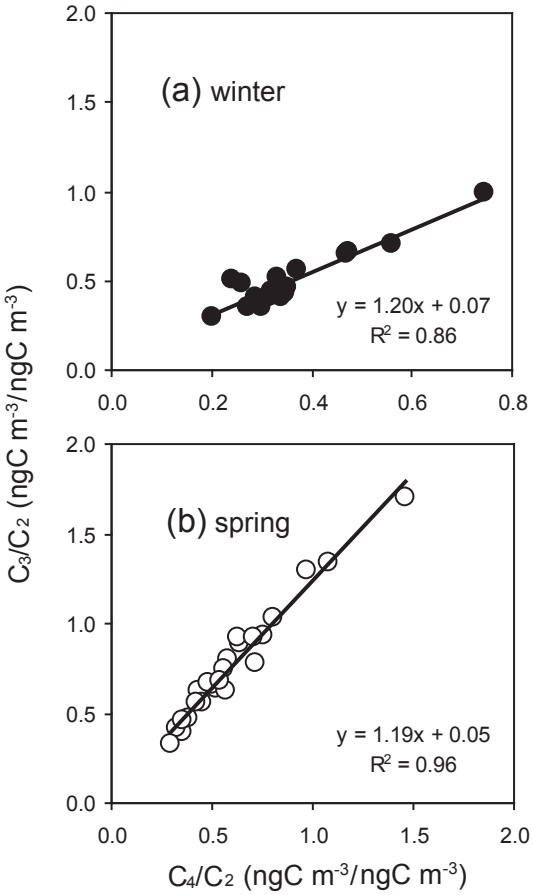

Fig. 4. Concentration ratios of oxalic acid (C_2) to malonic (C_3) and succinic (C_4) acids in PM_{10} from Baoji City during winter and spring.

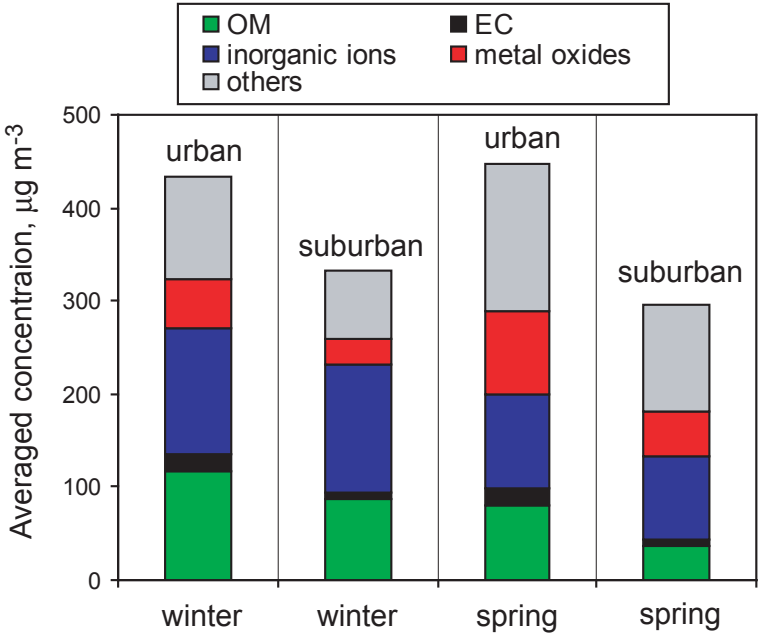

Fig. 5. Concentrations of major components determined in the PM_{10} of Baoji City (data of inorganic ions are cited from Wang et al., 2009a).

ACPD
10, 6895–6921, 2010

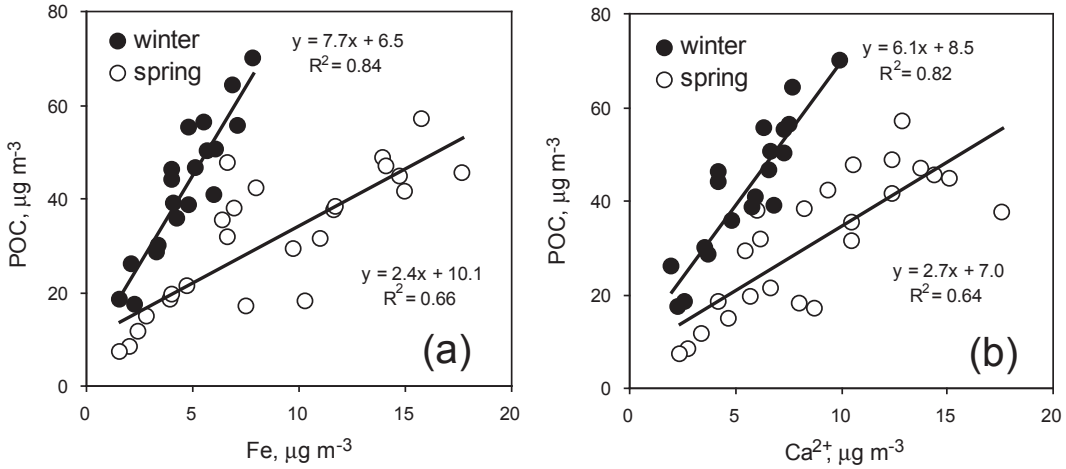

Fig. 6. Correlation of primary organic carbon (POC) with Fe and Ca^{2+} in the PM_{10} of Baoji City.

ACPD
10, 6895–6921, 2010

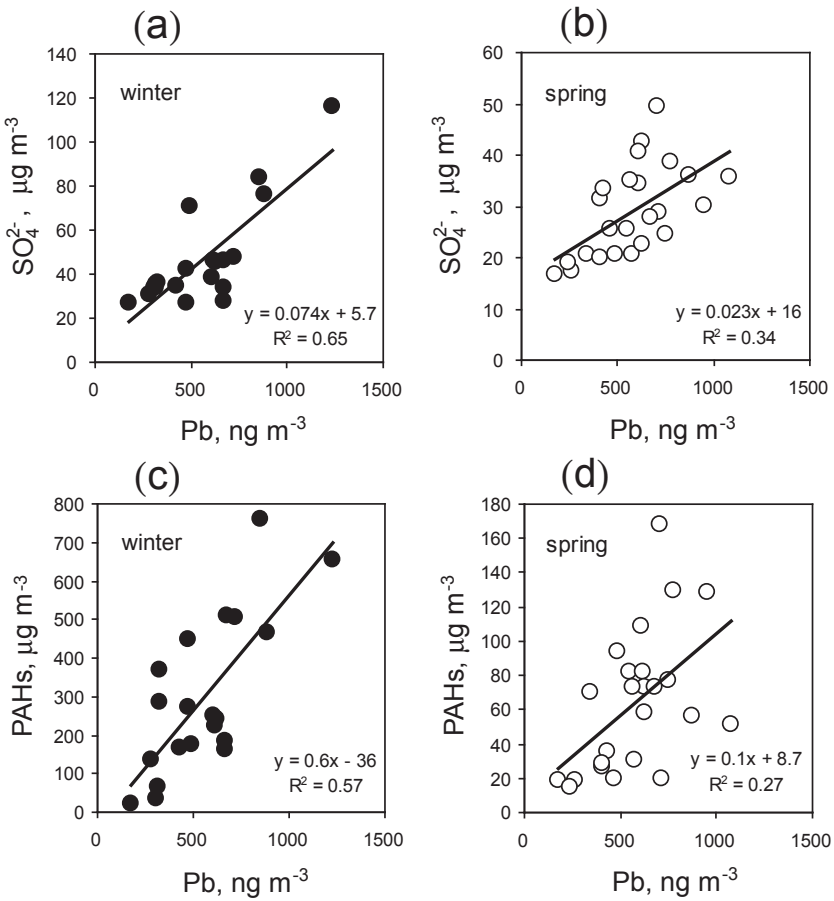

Fig. 7. Correlation of Pb with sulfate and PAHs in the PM_{10} of Baoji city during winter and spring (sulfate data are cited from Wang et al., 2009a, and PAH data are cited from Xie et al., 2009).

ACPD
10, 6895–6921, 2010

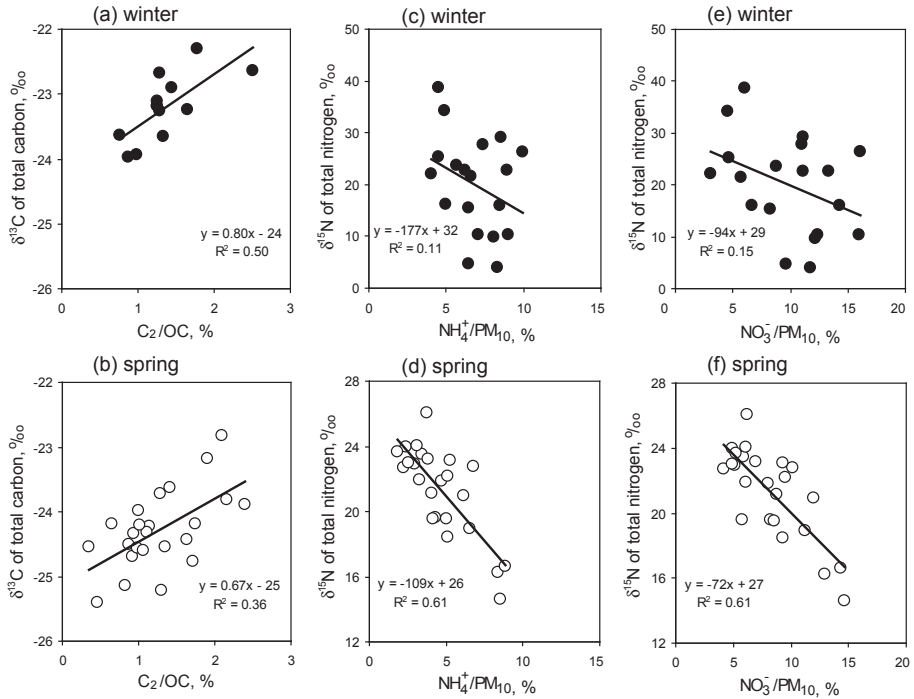

Fig. 8. Correlations of $\delta^{13}C$ of TC with C_2/OC (**a** and **b**) and $\delta^{15}N$ of TN with NH_4^+/PM_{10} (**c** and **d**) and NO_3^-/PM_{10} (**e** and **f**) during winter and spring (Due to instrument problem, the $\delta^{13}C$ data for a few winter samples are unavailable).

ACPD
10, 6895–6921, 2010